

Flow angle from intermediate mass fragment measurements

F. Rami¹, P. Crochet², R. Donà³, B. de Schauenburg¹, P. Wagner¹, J.P. Alard⁴,
 A. Andronic⁵, Z. Basrak⁶, N. Bastid⁴, I. Belyaev⁷, A. Bendarag⁴, G. Berek⁹, D. Best²,
 R. Čaplar⁶, A. Devismes², P. Dupieux⁴, M. Dželalija⁶, M. Eskef¹², Z. Fodor⁹, A. Gobbi²,
 Y. Grishkin⁷, N. Herrmann², K.D. Hildenbrand², B. Hong¹³, J. Kecskemeti⁹,
 M. Kirejczyk¹⁰, M. Korolija⁶, R. Kotte⁸, A. Lebedev^{7,11}, Y. Leifels², H. Merlitz¹²,
 S. Mohren¹², D. Moisa⁵, W. Neubert⁸, D. Pelte¹², M. Petrovici⁵, C. Pinkenburg²,
 C. Plettner⁸, W. Reisdorf², D. Schüll², Z. Seres⁹, B. Sikora¹⁰, V. Simion⁵,
 K. Siwek-Wilczyńska¹⁰, G. Stoicea⁵, M. Stockmeir¹², M. Vasiliev¹¹, K. Wisniewski²,
 D. Wohlfarth⁸, I. Yushmanov¹¹, A. Zhilin⁷

(FOPI Collaboration)

¹*Institut de Recherches Subatomiques, IN2P3-CNRS, Université Louis Pasteur, Strasbourg, France*

²*Gesellschaft für Schwerionenforschung, Darmstadt, Germany*

³*Istituto Nazionale di Fisica Nucleare, Legnaro, Italy*

⁴*Laboratoire de Physique Corpusculaire, IN2P3-CNRS, Université Blaise Pascal, Clermont-Ferrand, France*

⁵*Institute for Physics and Nuclear Engineering, Bucharest, Romania*

⁶*Ruđer Bošković Institute, Zagreb, Croatia*

⁷*Institute for Theoretical and Experimental Physics, Moscow, Russia*

⁸*Forschungszentrum Rossendorf, Dresden, Germany*

⁹*Research Institute for Particles and Nuclear Physics, Budapest, Hungary*

¹⁰*Institute of Experimental Physics, Warsaw University, Warsaw, Poland*

¹¹*Russian Research Institute "Kurchatov", Moscow, Russia*

¹²*Physikalisches Institut der Universität Heidelberg, Heidelberg, Germany*

¹³*Korea University, Seoul, Korea*

Abstract

Directed sideward flow of light charged particles and intermediate mass fragments was measured in different symmetric reactions at bombarding energies from 90 to 800 AMeV. The flow parameter is found to increase with the charge of the detected fragment up to $Z = 3 - 4$ and then turns into saturation for heavier fragments. Guided by simple simulations of an anisotropic expanding thermal source, we show that the value at saturation can provide a good estimate of the flow angle, Θ_{flow} , in the participant region. It is found that Θ_{flow} depends strongly on the impact parameter. The excitation function of Θ_{flow} reveals striking deviations from the ideal hydrodynamical scaling. The data exhibit a steep rise of Θ_{flow} to a maximum at around 250 – 400 AMeV, followed by a moderate decrease as the bombarding energy increases further.

Keywords : Heavy-ion collisions, Reaction plane, Directed sideward flow, Flow parameter, Flow angle, Expanding thermal source, hydrodynamical scaling.

PACS numbers : 25.70.-z,25.75.Ld

I. INTRODUCTION

The emergence and development of a collective expansion motion in the course of an energetic heavy-ion collision reflects the response of the nuclear system to the internal pressure built-up at the interface of the interacting nuclei. Thus, experimental investigations of this phenomenon are expected to provide information about the compressibility coefficient characterizing the nuclear equation-of-state which is one of the major objectives in nuclear physics research. This has generated a widespread interest in this subject which is currently the object of intensive experimental activities [1] over a broad range of bombarding energies going from the region where a possible liquid-gas phase transition might occur to the ultra-relativistic energy domain where the transition to the quark gluon plasma is expected to take place.

In finite impact parameter collisions, because of the presence of cold spectator remnants the expanding nuclear matter in the hot and dense central region is deflected sideways along a preferential emission direction in the reaction plane. The most natural experimental observable to characterize this effect is the flow angle, Θ_{flow} , *i.e.* the angle between the direction of the collective sideward motion and the longitudinal beam axis. This observable is of relevance not only because of its sensitivity to the stiffness of the nuclear matter equation-of-state, but its knowledge is also essential in other measurements such as the extraction of the squeeze-out signal around the flow axis [2–4] and two-particle interferometry [5]. Its determination requires the use of “ 4π ” detectors capable of global event reconstruction.

The sideward flow can be characterized using the transverse momentum analysis method [6]. The latter method allows one to extract the so-called “flow parameter”, F_S , which is defined as the slope at mid-rapidity of the average in-plane transverse momentum as a function of the rapidity. This observable is by definition representative of the highly excited and compressed central region. It has also the advantage that uncertainties on the reaction plane determination due to finite number of particle effects and detector biases can be accounted for by introducing an appropriate correction factor [6,7]. An inherent

problem in this method is that the flow parameter does not reflect only the collective behaviour but it is also sensitive to the random thermal motion of the emitted particles. In the absence of thermal fluctuations the scaled flow parameter $F_S^{(0)} = F_S/p_p^{\text{c.m.}}$, where $p_p^{\text{c.m.}}$ is the projectile center-of-mass (c.m.) momentum per nucleon, is a measure of the flow angle ($F_S^{(0)} = \tan(\Theta_{\text{flow}})$), while in the presence of a large thermal motion the value of $F_S^{(0)}$ might be significantly lower than $\tan(\Theta_{\text{flow}})$. It follows thereby that intermediate mass fragments (IMFs), which are less subjected to thermal fluctuations than do lighter particles, are expected to be strongly aligned along the flow direction. This effect was first observed by the Plastic Ball group [8] and confirmed later on in several experiments [4,9–13]. Recently, quantitative measurements of IMF sideward flow in the Kr+Au reaction at 200 AMeV have shown that the flow parameter increases with the size of the detected particle and reaches a constant limiting value for fragments with masses $4 \leq A \leq 12$ [11]. These considerations underscore the importance of accurate measurements of the flow parameter of IMFs, in particular at beam energies of a few hundred AMeV where IMFs are copiously produced [12,14–16].

Many interesting processes might simultaneously contribute to the observed flow : the release of compressional energy [17], the thermal pressure [18], the momentum dependence of the nuclear force [19,20] and the in-medium nucleon-nucleon cross sections [21]. Systematic studies by varying the bombarding energy and the system size are needed to disentangle the different contributions of these effects since they are expected to exhibit different dependences on the initial conditions.

In the present paper we report on detailed experimental results of the flow parameter of light charged particles and IMFs measured in different symmetric reactions, Ru+Ru, Xe+CsI and Au+Au, at beam energies between 90 AMeV and 800 AMeV. We show that an accurate estimate of the mean flow angle can be obtained from the observed flow parameter of heavy IMFs. Then, by applying this idea we investigate the dependences of the flow angle as a function of the collision impact parameter and the bombarding energy.

II. EXPERIMENTAL SETUP

The experimental results reported in this paper were obtained in a series of experiments carried out using the FOPI detector [22] at the SIS accelerator facility of GSI-Darmstadt. Several symmetric reactions at beam energies going from 90 AMeV to 1.9 AGeV were investigated. Here, we will present data for the following systems : Ru on Ru and Xe on CsI at $E = 400$ AMeV and Au on Au at $E = 90, 100, 120, 150, 250, 400, 600$ and 800 AMeV. The beam intensities were typically 10^5 ions/s. The target thickness was between 100 mg/cm^2 (at the lowest incident energy) and 400 mg/cm^2 (at the highest energy), corresponding to an interaction length going from 0.5% to 2% . Data at 600 and 800 AMeV were obtained from the first generation of FOPI experiments using the Phase I setup, while the lower beam energy data were taken more recently with the Phase II configuration of the FOPI detector. Details about the FOPI apparatus and its performances have been reported in previous publications [22,23]. Here, we recall briefly some of the sub-detector components of particular interest in the present analysis.

In its Phase I configuration [22], the FOPI detector consisted of a highly segmented Forward Wall of 764 plastic scintillators, divided into an external (512 strips) and an internal (252 scintillator paddles of trapezoidal shape) components. To identify the slow heavy fragments stopped in the external wall an ensemble of 16 large gas ionisation chambers with a total of 128 anodes of individual readout, positioned in front of the external wall, was also used. For the same purpose the inner part was supplemented with a shell of 60 thin (2 mm) plastic scintillator paddles. The whole setup covered the laboratory polar angles, Θ_{lab} , from 1.2° to 30° over the full azimuth. This device allowed us, event by event, to identify the nuclear charge and measure the vector velocities of most of the light charged particles and IMFs (up to $Z = 12$) emitted in the forward c.m. hemisphere. In phase II [23] experiments, a cylindrical drift chamber CDC mounted inside a superconducting solenoid was used at backward angles ($\Theta_{\text{lab}} = 30^\circ - 150^\circ$). Pions, protons and deuterons were identified in the CDC by means of their mean energy loss $\langle dE/dx \rangle$ and their laboratory momentum,

obtained from the curvature of the particle tracks in the field of a 0.6 T strength. The high granularity of the setup allowed high multiplicity events to be measured with a negligible multi-hit rate. The apparatus ensured also a very good azimuthal symmetry which is an important feature for the study of the flow phenomenon. As the main objective in this work was to extract information on the sideward flow of IMFs, our analysis was based mainly on the data from the forward sub-detectors. The CDC was used only for the purpose of event characterization, as we will see in the next section.

All data presented in this paper were obtained from the analysis of events taken under the “central trigger” condition [22]. The latter was defined by adjusting the charged particle multiplicity to a value which corresponds to impact parameters less than $\sim 2/3$ of the maximum impact parameter. At each bombarding energy, samples of about 10^5 to 10^6 of such events were recorded. This large amount of available events allowed us to extract high statistics data in particular for IMFs.

III. EVENT CHARACTERISATION

To extract quantitative information on flow phenomena from the data, one requires a good event characterization both in impact parameter and azimuth of the reaction plane.

In order to classify the measured events according to their degree of centrality, we have employed the standard method based on the correlation between the multiplicity of the emitted particles and the impact parameter. The event multiplicity was extracted as the number of charged particles detected per event in both the outer part (from 7° to 30°) of the forward scintillator wall and the CDC. For Au+Au at 600 and 800 AMeV where the CDC was not operational, the event multiplicity was restricted only to charged particles measured by the outer part of the scintillator wall. In the following, the event multiplicity will be labelled MUL when the CDC is included and PMUL otherwise. The measured event multiplicity distributions exhibit the typical plateau for intermediate values followed by a rapid fall off for the highest multiplicities [14,15]. These distributions were divided into five

intervals, in accordance to the procedure introduced in previous works [15,24]. The highest multiplicity bin, named MUL5 (or PMUL5) starts at half the plateau value and the remaining multiplicity range was divided into four equally spaced intervals, named MUL1 to MUL4 (or PMUL1 to PMUL4). Most of the results which will be presented in this paper deal with the MUL4 (or PMUL4) event class corresponding to an average geometrical impact parameter of ~ 3.5 fm (for the Au+Au reaction). As we will see, this centrality bin lies in the region where the sideward flow reaches its maximum [13,14]. The corresponding cross sections and mean geometrical impact parameters (obtained by assuming a sharp-cut-off approximation) are given in Tab. I and Tab. II. Note in passing that the value of the reduced impact parameter is nearly the same in all cases which will allow direct comparisons of the experimental results obtained for different systems and at different bombarding energies.

To reconstruct the reaction plane, we have used the transverse momentum analysis method [6]. In order to remove autocorrelation effects, the azimuth of the reaction plane was estimated for each particle i in a given event as the plane containing the vector \vec{Q}^i and the beam axis where \vec{Q}^i is calculated from the transverse momenta \vec{p}_t^j of all detected particles except the particle of interest i

$$\vec{Q}^i = \sum_{\substack{j=1 \\ j \neq i}}^M \omega^j (\vec{p}_t^j + m^j \vec{v}_b^j). \quad (1)$$

M is the multiplicity of the event and $\omega^j = 1$ if $y^{(0)} > \delta$, -1 if $y^{(0)} < -\delta$ and 0 otherwise. $y^{(0)}$ is the j^{th} particle rapidity divided by the projectile rapidity in the c.m. system. The parameter δ , chosen equal to 0.5 , was introduced in order to remove the contributions of mid-rapidity particles which have a negligible correlation with the reaction plane. According to Ref. [25], a boost velocity $\vec{v}_b^j = \vec{p}_t^j / (m^{\text{sys}} - m^i)$ (m^i is the mass of particle i and m^{sys} is the sum of the projectile and target masses) was applied to each particle j in order to take into account the effects of momentum conservation due to the exclusion of the particle of interest i . In order to estimate the accuracy on the reaction plane determination, due to finite number of particle effects and detector biases, we have used the method described in reference [6] which consists in randomly subdividing each event into two and calculating on

average the half difference in azimuth, $\Delta\Phi_R$, between the reaction planes extracted from the two sub-events. $\Delta\Phi_R$ gives an estimate of the dispersion of the reconstructed reaction plane with respect to the true one [6]. The results are displayed in Tab. I and Tab. II in terms of the standard deviation width $\sigma(\Delta\Phi_R)$ extracted from a gaussian fit to the $\Delta\Phi_R$ distributions. As can be seen, the reaction plane is, in all cases, rather well estimated, with a precision which varies typically from $\simeq 22^\circ$ to $\simeq 46^\circ$ depending upon the system and the incident energy. All data subsequently presented in this paper are corrected for these uncertainties on the reaction plane determination.

IV. EXPERIMENTAL RESULTS AND DISCUSSION

In the framework of the transverse momentum method [6], the sideward flow is quantified by plotting the mean in-plane transverse momentum per nucleon $\langle p_x \rangle$ as a function of the rapidity. For each particle, the quantity $\langle p_x \rangle$ is obtained by projecting its transverse momentum \vec{p}_t onto the reaction plane (the x direction is defined to be in the reaction plane). The reaction plane is reconstructed by removing autocorrelation effects as described in the previous section. In the present work, the data have been expressed in terms of scale invariant (dimensionless) quantities in order to avoid trivial scaling with the incident beam energy [26]. In what follows, scaled quantities will be indicated by the index (0) : $\langle p_x^{(0)} \rangle = \frac{\langle p_x \rangle}{p_p^{cm}}$ will denote the mean in-plane transverse momentum per nucleon $\langle p_x \rangle$ scaled to the projectile momentum per nucleon p_p^{cm} in the c.m. system and $y^{(0)} = \frac{y^{cm}}{y_p^{cm}}$ will refer to the c.m. particle rapidity y^{cm} normalized to the c.m. rapidity y_p^{cm} of the system.

Displayed in Fig. 1 are representative examples of $\langle p_x^{(0)} \rangle$ versus $y^{(0)}$ plots for the three reactions Au+Au, Xe+CsI and Ru+Ru, all at a beam energy of $E = 400$ AMeV. The data belong to the multiplicity bin MUL4 where, as outlined earlier, the directed sideward flow is close to its maximum. The $\langle p_x^{(0)} \rangle$ values have been divided by the mean cosine of $\Delta\Phi_R$ in order to take into account the resolution of the reaction plane determination. This has been done according to the method recently proposed by Ollitrault [7]. The values of

$\langle \cos(\Delta\Phi_R) \rangle$ are given in Tab. I and Tab. II. The small statistical uncertainties (smaller than the symbol sizes for $Z = 1$ and $Z = 2$ particles) on the experimental points, in particular for IMFs, illustrate the high statistics recorded in the present work. For the Ru+Ru reaction, the data for fragments with $Z > 4$ are subjected to relatively large statistical errors. There are two reasons for that : i) for this system only half of the available statistics was used and ii) the production yields of IMFs are lower in lighter systems. The plots of Fig. 1 were obtained from the analysis of the data taken by the sub-detector components composing the forward Wall (see section II), allowing IMF measurements. This is the reason why the plots of Fig. 1 are shown only in the forward hemisphere in the c.m. frame (positive c.m. rapidities). It is worth recalling that the forward Wall provides an individual element identification of light charged particles and IMFs (up to $Z = 12$) along with velocity measurements. Thus, the $\langle p_x^{(0)} \rangle$ *versus* $y^{(0)}$ distribution measured for a given fragment includes the contributions of all associated isotopes. It should be, however, stressed that the lack of mass identification does not affect the $\langle p_x^{(0)} \rangle$ quantity as it is directly derived from the measured velocities without any assumption on the mass of the particle.

As shown in Fig. 1, the measured $\langle p_x^{(0)} \rangle$ *versus* $y^{(0)}$ distributions exhibit the typical S-shape behavior [6,27] reflecting the transfer of momentum between the backward and forward hemispheres. The linear part of the S-shaped curve is representative of the flow in the participant region, the so-called side-splash effect, while the fall-off observed at high rapidities is caused by the bounce-off effect [28,29]. It is customary to quantify the magnitude of the participant flow as the slope of the $\langle p_x^{(0)} \rangle$ *versus* $y^{(0)}$ curve at mid-rapidity [27]

$$F_S^{(0)} = d \langle p_x^{(0)} \rangle / dy^{(0)} \Big|_{y^{(0)} \simeq 0} \quad (2)$$

In practice, we extracted this quantity $F_S^{(0)}$ (known as “flow parameter” in the literature) by fitting a polynomial function of the form $a + F_S^{(0)} \times y^{(0)} + c \times (y^{(0)})^3$ to the data. The fit was restricted to the linear branch of the S-shaped curve. We have verified that reasonable changes of the limits of the $y^{(0)}$ range where the fit is applied, lead to the same values of $F_S^{(0)}$ within the statistical error bars. It is worth to notice that the influence of momentum

conservation effects on the flow parameter was found to be very weak (less than a few %). More details on the fitting procedure can be found in Ref. [3,4].

Before presenting the results, let us briefly comment on the influence of the biases introduced by our apparatus on the measured values of the flow parameter. To evaluate these effects, we performed detailed simulations where theoretical events were passed through the FOPI detection filter including geometrical cuts and energy thresholds. The theoretical events were obtained from Quantum Molecular Dynamics (QMD) model calculations using the so-called IQMD version [30,31] which yields generally a quite good agreement with the sideward flow data [32,33]. We estimated the effects of detector cuts by comparing the flow parameter calculated with and without including the experimental filter. Because of limited statistics (we used samples of a few hundred IQMD events per impact parameter unit), this could be done accurately only for light particles. We found that the $F_S^{(0)}$ observable is mainly affected by the $\Theta_{\text{lab}} = 30^\circ$ cut. The results indicate that acceptance effects depend on the fragment charge, the collision centrality and the beam energy. For MUL4 events at an incident energy of $E = 250$ AMeV, $F_S^{(0)}$ was found to be biased down by about 30% and 10% for $Z = 1$ and $Z = 2$ particles, respectively. For heavier fragments, these effects are expected to be much lower as the $\Theta_{\text{lab}} = 30^\circ$ cut has a weaker influence on IMFs. This will be illustrated later on (Fig. 5) using more simple simulations based on the decay of an expanding thermal source.

A. Centrality dependence of the flow parameter

Figure 2 shows the dependence of the scaled flow parameter measured for Au(400 AMeV)+Au as a function of the collision impact parameter. Error bars correspond to statistical uncertainties multiplied by $\sqrt{\chi^2}$ to take into account the uncertainty from the polynomial fit to data. The impact parameter was obtained from the measured cross sections ($b_{geo} = \sqrt{\sigma/\pi}$) assuming a sharp-cut-off approximation. The flow parameter $F_S^{(0)}$ is presented here in the form of a coalescence invariant quantity [33–35], *i.e.* including

the contributions of all detected particles each weighted by its measured charge.

The results exhibit a maximum of the sideward flow around $b = 4.8$ fm. The observed trend is qualitatively consistent with the earlier results [27] reported by the Plastic Ball group at the same incident energy. It can be intuitively understood from the expectation that the flow parameter should be zero at $b = 0$, for symmetry reasons, and must tend also towards zero in peripheral collisions. The value of $F_S^{(0)}$ at maximum (~ 0.38) is, within acceptance effects, in good agreement with the data of the Plastic Ball group and those more recently published by the EOS Collaboration [10].

B. Fragment charge dependence of the flow parameter

The fragment charge dependence of the flow parameter is depicted in Fig. 3 for Au+Au reactions at different bombarding energies. Error bars correspond to statistical uncertainties multiplied by $\sqrt{\chi^2}$. The data are not corrected for the distortions introduced by the FOPI apparatus. The influence of detector cuts on the measured flow parameters has been already discussed. Qualitatively, the data exhibit the same pattern at all five beam energies, characterized by a gradual increase of $F_S^{(0)}$ with the charge of the detected particle followed by a clear tendency to level-off above a certain value of Z . With increasing beam energies, the saturation appears at lower Z values. This is illustrated by the curves representing the results of a fit with a Fermi function to the data.

A similar behaviour has been recently reported in the Kr + Au reaction at 200 AMeV where the flow parameter was found to reach a constant limiting value for fragments with masses $4 \leq A \leq 12$ [11]. It is worth-while mentioning that this trend has been also seen for the squeeze-out effect [3,36] and seems to be typical for all flow observables [13].

The increasing strength of the sideward flow with the fragment size was observed for the first time [8] by the Plastic Ball group for Au(200 AMeV)+Au reactions and confirmed, since then, in several experiments [4,9–13]. This phenomenon was predicted by hydrodynamical models [37] where collective effects were found to be much more visible for heavier

mass fragments. QMD calculations also yield larger flow for heavier fragments [38]. This large flow carried by fragments is of particular interest because of its enhanced sensitivity to the parametrisation of the nuclear equation-of-state used in dynamical model calculations [33,38,39].

It can be also understood from the interplay between collective and thermal (random) motions. In an idealized picture in which nucleons and fragments are emitted from a common expanding thermalized source, heavy fragments are less subjected to thermal fluctuations than do lighter particles. Thermal fluctuations are governed by the thermal energy which is independent of the mass of the particle, while the collective expansion energy increases linearly with the mass and is, therefore, better reflected in heavier fragments. Thus, it is easy to understand, within this simple picture, that in the presence of thermal fluctuations the apparent flow angle that one can extract from the flow parameter $\Theta_{\text{flow}}^{\text{app}} = \arctan(F_S^{(0)})$ is lower than the effective flow angle. The nearly constant value observed in the flow parameter of heavy fragments (Fig. 3) can be attributed to the fact that above a certain mass (or charge) the emitted fragments are only very little affected by the random thermal motion so that their apparent flow angles are expected to be very close to the effective flow angle. That is the idea that we will exploit below (section IV.D) in order to extract an estimate of the flow angle from the data.

It should be mentioned that it was shown in Ref. [34] that the increase of the sideward flow with fragment size can be also described by a simple momentum space coalescence prescription providing a transverse momentum cut of 0.2 AGeV is imposed.

C. System size dependence of the flow parameter

In Fig. 4, the normalised flow parameter $F_S^{(0)}$ as a function of the charge of the detected fragment is displayed for the three reactions under study. The flow parameter is divided here by the quantity $A_P^{1/3} + A_T^{1/3}$, where A_P and A_T denote the mass of, respectively, the projectile and target nuclei. Two observations can be readily made from the examination of this figure.

First, the dependence of the flow parameter on the fragment charge measured in Ru+Ru and Xe+CsI reactions follows the same trend as observed in the heavier system Au+Au. Second, the projectile-target mass dependence of $F_S^{(0)}$ is consistent, within statistical uncertainties, with the $A_P^{1/3} + A_T^{1/3}$ empirical scaling rule introduced recently by the EOS collaboration [40]. The origin of this scaling rule is not yet well understood. It might be attributed, in a hydrodynamical picture, to the fact that for collisions with velocities well above that of sound, the pressure built-up should scale with collision length or time [40].

D. Extraction of the flow angle from IMF measurements

As outlined in the introduction, the most natural observable characterizing the sideward deflection of the nuclear matter emitted in non-zero impact parameter collisions is the flow angle *i.e.* the angle between the direction of the collective sideward motion and the longitudinal beam axis. Indeed in contrast to the flow parameter, Θ_{flow} is a measure of the overall emission direction of all particles belonging to a given event and is not affected by thermal fluctuations. It follows therefore that the determination of this observable, because of its greater sensitivity, should help to better understand the origin of the flow and disentangle the different phenomena that may contribute to the observed effect. The knowledge of Θ_{flow} is, on the other hand, of great importance in the investigation of other phenomena such as the out-of-plane squeeze-out effect [2–4] and two-particle interferometry [5].

Several methods were introduced to reconstruct this observable in high energy heavy-ion experiments. The sphericity method [41], based on the diagonalization of the momentum flow tensor, allows the extraction of the flow angle as well as two aspects ratios characterizing the event shape (assumed to be ellipsoidal). This procedure has the advantage that it provides an event-by-event shape characterization. It deals, however, with the overall emission pattern including the spectator component. Furthermore, the sphericity analysis is strongly affected by the distortions due to the effects of finite number of particles [42]. An alternative shape analysis method, where the contribution of the spectator matter can be removed, was

proposed by Gosset et al [43]. The flow angle is adjusted, within this method, by fitting a simple anisotropic gaussian distribution to the triple differential momentum distributions of particles detected in the participant region. This procedure is nevertheless reliable only in the case of low impact parameter collisions where the contribution of the spectator matter is not very important [44].

We propose in the present article a new method which exploits the saturation observed in the dependence of the flow parameter as a function of the fragment charge (Fig. 3 and 4). As discussed earlier this saturation is due to the fact that IMFs are much more aligned along the flow direction than do lighter particles : “IMFs go with the flow” [39,45]. One expects therefore that if the phase space region occupied by IMFs is sufficiently elongated then their apparent flow angle $\Theta_{\text{flow}}^{\text{app}}$ should give a good measure of the effective flow angle.

To investigate more quantitatively this idea, we have performed Monte-Carlo simulations based on an anisotropically expanding thermal source calculations, where particles with different masses share the same thermal energy but their collective energy is proportional to their mass. We assume that, at the freeze-out stage of the collision, the nuclear system is in local thermal equilibrium, *i.e.* same temperature throughout the entire volume of the source. The latter is considered as a cylinder, in configuration space, whose principal axis coincides with the flow axis. The flow angle is introduced as a free parameter, $\Theta_{\text{flow}}^{\text{input}}$, in the simulations. Particles are generated one by one independently of the influence on each other. The momentum of a given fragment is considered as resulting from the superposition of a purely collective component (common velocity field to all fragments) on the top of a thermal motion¹

$$\vec{p} = \vec{p}^{\text{th}} + \vec{p}^{\text{coll}} \quad (3)$$

The random thermal component \vec{p}^{th} is assumed to obey a Maxwellian distribution

$$M(p^{\text{th}}, m) = p^{\text{th}2} e^{-\sqrt{m^2 + p^{\text{th}2}}/T} \quad (4)$$

¹details about the simulations can be found in Ref. [3].

where m is the mass of the fragment and T is the temperature of the source.

The collective component \vec{p}^{coll} is calculated assuming that at the moment of the explosion, the expansion velocity of a fragment increases linearly along the spatial coordinates towards the surface of the freeze-out volume

$$v_i^{\text{coll}} = \left. \frac{r_i}{q_i} \sqrt{\frac{2 \langle E_i^{\text{coll}}/A \rangle}{931.8}} \right\}_{i=x,y,z} \quad (5)$$

The fragment positions r_i ($i = x, y, z$), expressed in the source reference frame, are randomly determined inside the cylindrical volume of the source assuming a uniform density at the freeze-out. $\langle E_i^{\text{coll}}/A \rangle$ is the mean collective energy per nucleon along the direction i and q_i is a normalization constant given by [46]

$$q_i = \left. \sqrt{\frac{\sum_{j=1}^N r_{i,j}^2}{N}} \right\}_{i=x,y,z} \quad (6)$$

where N is the number of the particles generated in the simulations.

It is worth pointing out that the generation of full events is beyond the scope of the present simulations. Our purpose here is to simulate in a very simple way the phase space distributions of fragments of different masses emitted in the mid-rapidity region. The aim is to explore whether the apparent flow angle provided by IMF sideward flow data can be considered as an accurate measure of the the effective flow angle.

The simulations were carried out for semi-central events in the MUL4 event bin at an incident energy of $E = 150$ AMeV where IMFs are copiously produced [13,14]. We have used the following values as input parameters : $T = 20$ MeV, $\langle E_x^{\text{coll}}/A \rangle = \langle E_y^{\text{coll}}/A \rangle = 3.4$ MeV, $\langle E_z^{\text{coll}}/A \rangle = 8$ MeV and $\Theta_{\text{flow}}^{\text{input}} = 27.5^\circ$. Within this set of parameters, we could achieve a quite reasonable reproduction [3] of the $dN/p_t dp_t$ distributions measured in the mid-rapidity region. The azimuthal anisotropy due to the squeeze-out effect [3,36] was neglected (*i.e.* we assumed that $\langle E_x^{\text{coll}}/A \rangle = \langle E_y^{\text{coll}}/A \rangle$). The value of $\Theta_{\text{flow}}^{\text{input}}$ used in the calculations was taken equal to the apparent flow angle measured for $Z = 7$ fragments. The temperature parameter was found to affect only weakly the flow parameter of IMFs (less

subject to thermal fluctuations). Its value was constrained to match the experimental flow parameter of $Z = 2$ particles.

In Fig. 5 we compare the experimental data (open circles), expressed in terms of the apparent flow angle versus the fragment charge, to the outcome of the simulations with (stars) and without (triangles) taking into account the detector filter [47]. In the calculations, the mass of $A \geq 4$ particles was assumed to be equal to twice their charge $A = 2 \times Z$. For $A \leq 3$ particles, the experimental isotopic ratios [48] were taken into account. As it can be seen, the filtered calculations supply a fairly good quantitative reproduction of the observed charge dependence of the apparent flow angle. Note in particular that the saturation seen in the data for the heaviest fragments is also present in the simulations. As the particles become heavier, the value of the apparent flow angle converges toward the value of the effective flow angle $\Theta_{\text{flow}}^{\text{input}}$ (dotted line in Fig. 5) used as an input in the simulations. This strengthens the idea that a good estimate of the mean flow angle can be extracted from the present measurements of IMF sideward flow. It is also interesting to notice that the biases introduced by the FOPI apparatus do not affect significantly the apparent flow angle of IMFs. At the incident energy considered here ($E = 150$ AMeV), above $Z = 5$ (Fig. 5) filtered and unfiltered calculations give almost the same results.

E. Scaling properties of the flow angle

It is interesting to investigate now the dependences of the flow angle on the impact parameter and the incident energy. To this end, we applied the method described above to evaluate the flow angle from the data. Practically, to quantify the constant limiting value from the Z -dependence of the apparent flow angle, we calculated the average over the $\Theta_{\text{flow}}^{\text{app}}$ values measured for the heaviest fragments in the saturation region. The range of fragment charges included in the average, at each beam energy, is indicated by the shaded area in Fig. 3. The results are displayed in Fig. 6 for the Au+Au reaction. Error bars are the resulting uncertainties on the average value.

As is seen in the left-hand panel of Fig. 6 at an incident energy of $E = 400$ AMeV, the flow angle is found to depend strongly on the collision centrality. We observe a monotonic increase of Θ_{flow} with decreasing impact parameters. This trend is qualitatively in agreement with the predictions of several theoretical models [19,49,50]. The latter models predict that Θ_{flow} reaches 90° (with an oblate shape), in the limit of the most central collisions ($b \rightarrow 0$). This very interesting issue cannot, however, be directly addressed on the basis of the present data as the procedure used to evaluate Θ_{flow} is not reliable for low impact parameter collisions. For relatively central events ($b_{\text{geo}} \leq 3$ fm), the dispersion on the reconstructed reaction planes is dramatically large and the effect on the apparent flow angle becomes difficult to be accounted for. Investigations of c.m. polar angular distributions [14,51] are expected to be better suited for elucidating this still debated question concerning the flow pattern in highly central collisions.

The excitation function of the sideward flow was already investigated in several experiments [4,10,27,40,52]. However, in all these studies the sideward flow was expressed in terms of the flow parameter or the directed transverse momentum (p_x^{dir}) which are, in contrast to Θ_{flow} , subject to the fluctuations introduced by the thermal motion. Here, we report for the first time on the incident energy dependence of the flow angle. The latter observable being a measure of the “pure” collective motion, its evolution with the bombarding energy is expected to better reflect the collective response of the nuclear system under different conditions. The experimental results are presented in the right-hand panel of Fig.6 for the Au+Au reaction over a very broad energy range going from 90 to 800 AMeV. The data are shown for semi-central (MUL4 or PMUL4) events where the directed sideward flow is close to its maximum.

The observed trend (Fig. 6) is characterized by a steep rise of Θ_{flow} to a maximum at around $E = 250 - 400$ AMeV, followed by a moderate decrease as the bombarding energy increases further. This is in complete disagreement with the scaling behaviour, *i.e.* constant flow angle, expected from ideal-fluid hydrodynamics [26,49]. Quantitative calculations in the framework of one-fluid viscous hydrodynamics [49] have shown that Θ_{flow} scales with the

impact parameter almost independently of the incident energy (from 200 to 800 AMeV). It was also found in these calculations that the equation-of-state and the viscosity do not influence significantly the value of the flow angle. It seems therefore that, within this model, the flow angle is mainly governed by the collision geometry.

Deviations from scaling are visible in the data (Fig. 6) at both low and high incident energies. Such deviations are generally thought to signal [26] the presence of phenomena known to violate scaling such as the influence of the equation-of-state and possible phase transitions [26]. On the low energy end, the departure from scaling is particularly striking. One observes a drastic drop of the flow angle below 150 AMeV. This effect was already reported in an earlier publication where we have presented the excitation functions of the flow parameter [3]. It is probably caused by a transition from predominantly attractive to repulsive forces resulting in a liquid-to-vapour phase transition. A rough linear extrapolation toward lower incident energies leads to an intersection energy where the sideflow vanishes, the so-called balance energy, of about 54 AMeV. This value is somewhat lower than our previous evaluation in Ref. [3,4]. This is due to the fact that the data in Ref. [3] were corrected for the resolution of the reaction plane using the method of Ref. [6]. The latter method applied at low incident energies $E \leq 120$ AMeV, where the fluctuations on the reaction plane are relatively large, overestimates the correction factors and leads, therefore, to lower flow values [53].

Changes in the nuclear viscosity, η , might also contribute to the sudden change of Θ_{flow} at low energies. Below ~ 100 AMeV, η is relatively high because of the influence of the Pauli principle. With increasing energies, η is expected to drop allowing therefore for a fast (sudden) buildup of pressure. This was quantitatively investigated in reference [54] where realistic viscosities, derived from Uehling-Uhlenbeck equations, were used.

The origin of the smooth decline of Θ_{flow} observed at high bombarding energies (Fig. 6) is not yet clearly understood. It might be also attributed to a combination of several effects : the anisotropy of the nucleon-nucleon interaction, the excitation of resonances and possible changes in the stiffness of the equation-of-state [55]. Recent data from AGS [56]

and CERN/SPS [57,58] experiments at higher energies indicate relatively small sideward flow effects. An estimate of $\Theta_{\text{flow}} \sim 1/20\text{deg.}$ was reported from the Pb(158A GeV)+Pb data [57].

Overall, the rise and fall of the sideward flow, although it is not yet clearly understood, reflects certainly important changes in the properties of strongly interacting hot and dense hadronic matter. At the low energy end, the onset of flow is indicative of a reduced pressure in the system and hence might testify to a liquid-gas phase transition. Similarly, the fall of flow on the high energy side might also result from the possible transition towards the quark gluon plasma phase which is expected to soften the equation-of-state [55]. The present data deserve, therefore, to be further investigated in conjunction with the higher energy data from AGS and SPS experiments. First attempts along this line have started very recently [1].

V. SUMMARY AND CONCLUSION

In this work, a systematic study of the directed sideward flow of light charged particles and intermediate mass fragments was achieved with the FOPI detector at the SIS/ESR facility. Three symmetric reactions, Ru+Ru, Xe+CsI and Au+Au, were investigated at beam energies between 90 A MeV and 800 A MeV. The data were analysed according to the transverse momentum analysis method and corrections for the finite resolution of the reaction plane reconstruction were applied.

The flow parameter exhibits the expected correlation with the collision centrality with a well defined maximum at an impact parameter around $b = 4.8$ fm and vanishing sideflow at both the low and high b ends. Consistent with earlier results [40], the sideward flow scales according to the $A_P^{1/3} + A_T^{1/3}$ scaling rule.

The flow parameter is found to rise with the charge of the detected fragment up to $Z = 3 - 4$ and then turns into saturation for heavier fragments. This trend supports the concept of a collective motion and can be quantitatively accounted for by simple simulations based on an anisotropically expanding thermal source. Based on these simulations, we have

shown that the value of the flow parameter at saturation provides a good estimate of the flow angle Θ_{flow} in the participant region, offering therefore a new method to evaluate this observable in the beam energy range considered here. In contrast to the flow parameter, Θ_{flow} has the advantage to be unaffected by the influence of the thermal motion.

Applying this method, we have explored the dependences of the flow angle on both the collision centrality and the bombarding energy. In the impact parameter range ($b > 3$ fm) where this method is applicable, Θ_{flow} rises monotonically as the collision becomes more central. This trend is qualitatively in agreement with the predictions of several theoretical models [19,49,50]. The excitation function of Θ_{flow} reveals clear deviations from the flat dependence expected from an ideal hydrodynamical scaling. The data exhibit a steep rise of Θ_{flow} to a maximum at around 250 – 400 AMeV, followed by a moderate decrease as the bombarding energy increases further. On the low energy end, the departure from scaling is particularly striking. The flow angle drops drastically below 150 AMeV. This effect might be caused by a sudden decrease of the internal pressure due to the influence of the attractive mean field. A rough extrapolation toward lower incident energies leads to an estimate of the balance energy to about 54 AMeV. This value is consistent with the systematics of the balance energy [59]. The origin of the smooth decrease of Θ_{flow} observed above 400 AMeV is not yet clearly understood. It might be attributed to a combination of several effects : the anisotropy of the nucleon-nucleon interaction, the excitation of resonances and possible changes in the stiffness of the equation-of-state [55]. A quantitative evaluation of these effects would require detailed comparisons with the predictions of microscopic transport models. Further studies in conjunction with the higher energy data from AGS and SPS experiments should also shed some light on the mechanism responsible for the decline of flow at high incident energies.

ACKNOWLEDGEMENT

This work was supported in part by the French-German agreement between GSI and IN2P3/CEA and by the PROCOPE-Program of the DAAD.

REFERENCES

- [1] For recent reviews see, W. Reisdorf and H.G. Ritter, *Annu. Rev. Nucl. Sci.* **47** (1997) 663, J.Y. Ollitrault, *Nucl. Phys. A* **638** (1998) 195c.
- [2] H.H. Gutbrod, K.H. Kampert, B.W. Kolb, A.M. Poskanzer, H.G. Ritter, R. Schicker and H.R. Schmidt, *Phys. Rev. C* **42** (1990) 640.
- [3] P. Crochet, Thesis, Strasbourg University, France (1996) and XXXIV International Winter Meeting on Nuclear Physics, Bormio, Italy (1996), p.421.
- [4] P. Crochet *et al.*, FOPI Collaboration, *Nucl. Phys. A* **624** (1997) 755.
- [5] R. Kotte *et al.*, FOPI Collaboration, *Phys. Rev. C* **51** (1995) 2686.
- [6] P. Danielewicz and G. Odyniec, *Phys. Lett.* **157** B (1985) 146.
- [7] J.Y. Ollitrault, nucl-ex/9711003 (1997).
- [8] K.G.R. Doss *et al.*, *Phys. Rev. Lett.* **59** (1987) 2720.
- [9] S.G. Jeong *et al.*, FOPI Collaboration, *Phys. Rev. Lett.* **72** (1994) 3468.
- [10] M.D. Partlan *et al.*, *Phys. Rev. Lett.* **75** (1995) 2100.
- [11] M.J. Huang *et al.*, *Phys. Rev. Lett.* **77** (1996) 3739.
- [12] F. Rami *et al.*, FOPI Collaboration, XXXI International Winter Meeting on Nuclear Physics, Bormio (1993) p. 200.
- [13] F. Rami, Proceedings of “International Research Workshop on Heavy-Ion Physics at Low, Intermediate and Relativistic Energies using 4π Detectors” Poina-Brasov, Romania, October 7-14, 1996, World Scientific Publishing Co., 1997, p.160, edited by M.Petrovici, A.Sandulescu, D.Pelte, H.Stöcker and J.Randrup.
- [14] W. Reisdorf *et al.*, FOPI Collaboration, *Nucl. Phys. A* **612** (1997) 493.
- [15] J.P. Alard *et al.*, FOPI Collaboration, *Phys. Rev. Lett.* **69** (1992) 889.

- [16] N. Herrmann, Nucl. Phys. A **553** (1993) 739c.
- [17] W. Scheid, H. Müller and W. Greiner, Phys. Rev. Lett. **32** (1974) 741.
- [18] W.A. Friedmann, Phys. Rev. C **42** (1990) 667.
- [19] J. Aichelin *et al.*, Phys. Rev. Lett. **58** (1987) 1926.
- [20] C. Gale *et al.*, Phys. Rev. C **35** (1987) 1966.
- [21] N. Ohtsuka *et al.*, Nucl. Phys. A **490** 715 (1988).
- [22] A. Gobbi *et al.*, FOPI Collaboration, Nucl. Inst. Meth. A **324** (1993) 156.
- [23] J. Ritman *et al.*, FOPI Collaboration, Nucl. Phys. (Proc. Suppl.) B **44** (1995) 708.
- [24] K.G.R. Doss *et al.*, Phys. Rev. C **32** (1985) 116.
- [25] C.A. Ogilvie *et al.*, Phys. Rev. C **40** (1989) 2592.
- [26] A. Bonasera and L.P. Csernai, Phys. Rev. Lett. **59** (1987) 630.
- [27] K.G.R. Doss *et al.*, Phys. Rev. Lett. **57** (1986) 302.
- [28] H.A. Gustafsson *et al.*, Phys. Rev. Lett. **52** (1984) 1590.
- [29] H.H. Gutbrod, A.M. Poskanzer and H.G. Ritter, Rep. Prog. Phys. **52** (1989) 1267.
- [30] C. Hartnack, Thesis, Frankfurt University, Germany (1992).
- [31] C. Hartnack, J. Aichelin, H. Stöcker and W. Greiner, Phys. Lett. B **336** (1994) 131.
- [32] T. Wienold, Thesis, Heidelberg University, Germany (1993).
- [33] P. Crochet *et al.*, FOPI Collaboration, Nucl. Phys. A **627** (1997) 522.
- [34] S. Wang *et al.*, Phys. Rev. Lett. **74** (1995) 2646.
- [35] M.B. Tsang *et al.*, Phys. Rev. C **53** (1996) 1959.
- [36] N. Bastid *et al.*, FOPI Collaboration, Nucl. Phys. A **622** 573 (1997).

- [37] H. Stöcker, A.A. Ogloblin and W. Greiner, Z. Phys. A **303** (1981) 259.
- [38] G. Peilert *et al.*, Phys. Rev. C **39** (1989) 1402.
- [39] J. Zhang et C. Gale, Phys. Rev. C **51** (1995) 1425.
- [40] J. Chance *et al.*, Phys. Rev. Lett. **78** (1997) 2535.
- [41] M. Gyulassy, K.A. Frankel and H. Stöcker, Phys. Lett. B **110** (1982) 185.
- [42] P. Danielewicz and M. Gyulassy, Phys. Lett. B **129** (1983) 243.
- [43] J. Gosset *et al.*, Phys. Lett. B **247** (1990) 233.
- [44] N. Bastid *et al.*, FOPI Collaboration, GSI annual report 1998.
- [45] H.A. Gustafsson *et al.*, Mod. Phys. Lett. A **3** (1988) 1323.
- [46] J. Randrup, Comp. Phys. Comm. **77** (1993) 153.
- [47] S. Hölbling, FOPI Collaboration, program flf1f1 (available on request).
- [48] G. Poggi *et al.*, FOPI Collaboration, Nucl. Phys. A **586** 755 (1995).
- [49] W. Schmidt *et al.*, Phys. Rev. C **47** (1993) 2782.
- [50] P. Danielewicz, Phys. Rev. C **51** (1995) 716.
- [51] C. Roy *et al.*, FOPI Collaboration, Z. Phys. A **358** (1997) 73.
- [52] W.M. Zhang *et al.*, Phys. Rev. C **42** (1990) R491.
- [53] A.M. Poskanzer and S.A. Voloshin, Phys. Rev. C **58** (1998) 1671.
- [54] P. Danielewicz, Phys. Lett. B **146** (1984) 168.
- [55] D.H. Rischke, Nucl. Phys. A **610** (1996) 88c.
- [56] J. Barrette, E877 Collaboration, Phys. Rev. C **55** (1997) 1420.
- [57] H. Appelshäuser *et al.*, NA49 Collaboration, Nucl. Phys. A **638** (1998) 463c.

[58] H. Appelshäuser *et al.*, NA49 Collaboration, Phys. Rev. Lett. **80** (1998) 4136.

[59] A. Buta *et al.*, Nucl. Phys. A **584** (1995) 397.

TABLES

TABLE I. Measured cross section (σ), geometrical impact parameter (b_{geo}), reduced geometrical impact parameter (b_{geo}/b_{max}), accuracy on the determination of the reaction plane ($\sigma(\Delta\Phi_R)$) and the correction factors ($\langle \cos(\Delta\Phi_R) \rangle$) for the three reactions under study. The results are given for events in the MUL4 bin at an incident energy of $E = 400$ AMeV. The maximum impact parameter, b_{max} , was calculated assuming $r_0 = 1.20$ fm.

	Ru+Ru	Xe+CsI	Au+Au
σ (barn)	0.420	0.523	0.738
b_{geo} (fm)	2.83	3.12	3.61
b_{geo}/b_{max}	0.26	0.26	0.26
$\sigma(\Delta\Phi_R)$ (deg.)	34.24	31.09	22.4
$\langle \cos(\Delta\Phi_R) \rangle$	0.833	0.862	0.901

TABLE II. Measured cross section (σ), mean geometrical impact parameter (b_{geo} and b_{geo}/b_{max}), accuracy on the determination of the reaction plane ($\sigma(\Delta\Phi_R)$) and the correction factors ($\langle \cos(\Delta\Phi_R) \rangle$) for Au+Au collisions at different beam energies. The results are given for the MUL4 (PMUL4 for the 600 and 800 AMeV data) event class. b_{max} was calculated assuming $r_0 = 1.2$ fm.

E (AMeV)	90	120	150	250	400	600	800
σ (barn)	0.577	0.720	0.608	0.753	0.738	0.575	0.617
b_{geo} (fm)	3.75	3.98	3.53	3.68	3.61	3.44	3.58
b_{geo}/b_{max}	0.27	0.28	0.25	0.26	0.26	0.25	0.23
$\sigma(\Delta\Phi_R)$ (deg.)	46.2	39.03	33.7	24.7	22.4	24.8	28.8
$\langle \cos(\Delta\Phi_R) \rangle$	0.552	0.758	0.838	0.893	0.901	0.885	0.847

FIGURES

FIG. 1. Normalized mean in-plane transverse momentum per nucleon ($\langle p_x^{(0)} \rangle$) as a function of the normalized rapidity ($y^{(0)}$) for particles with charge $Z = 1$ (full squares), 2 (open triangles), 3 (dots), 4 (open squares), 5 (full triangles) and 6 (stars). The data are shown for Au+Au (a), Xe+CsI (b) and Ru+Ru (c) reactions for the same MUL4 centrality cut and at the same bombarding energy of $E = 400$ AMeV. They are corrected for fluctuations of the reaction plane. For the sake of clarity, an offset ($\text{const} = 0.7 \times (Z - 1)/10$) is applied to the data points corresponding to a given particle of charge Z . Error bars include statistical errors only.

FIG. 2. Dependence of the normalized flow parameter on the geometrical impact parameter. The data are shown at a bombarding energy of 400 AMeV. Error bars are statistical errors multiplied by $\sqrt{\chi^2}$. Geometrical impact parameters are deduced from the measured cross sections assuming a sharp-cut-off approximation.

FIG. 3. Normalized flow parameter *versus* the charge of the detected fragment. The data are shown for the Au+Au reaction at different beam energies, under the MUL4 or PMUL4 (for 600 and 800 AMeV) centrality cut. Error bars are statistical errors multiplied by $\sqrt{\chi^2}$. The solid lines are fits to the data using Fermi functions. The shaded area indicates the Z range used to extract the average flow angle (see section IV.E)

FIG. 4. Normalized flow parameter scaled to $(A_P^{1/3} + A_T^{1/3})$ *versus* the charge of the detected fragment. The results are shown for the three reactions under study at an incident energy of 400 AMeV. The MUL4 centrality cut was applied to all 3 reactions. Error bars are statistical errors multiplied by $\sqrt{\chi^2}$.

FIG. 5. Apparent flow angle *versus* the fragment charge for Au(150 AMeV)+Au semi-central (MUL4) collisions. Error bars take into account statistical errors only. The data (open circles) are compared to the results of anisotropic expanding thermal source model simulations with (stars) and without (triangles) the FOPI detector filter. The horizontal dotted line corresponds to the value of $\Theta_{\text{flow}}^{\text{input}} = 27.5^\circ$ used in the calculations. See text for more details.

FIG. 6. Left-hand panel : Mean flow angle as a function of the geometrical impact parameter. Data are shown for the Au+Au reaction at an incident energy of $E = 400$ AMeV. Right-hand panel : Mean flow angle as a function of the bombarding energy. Data are shown for Au+Au collisions under the MUL4/PMUL4 centrality cut corresponding to mean geometrical impact parameters in the range 3.5 - 4 fm (see Tab.2).

Figure 1

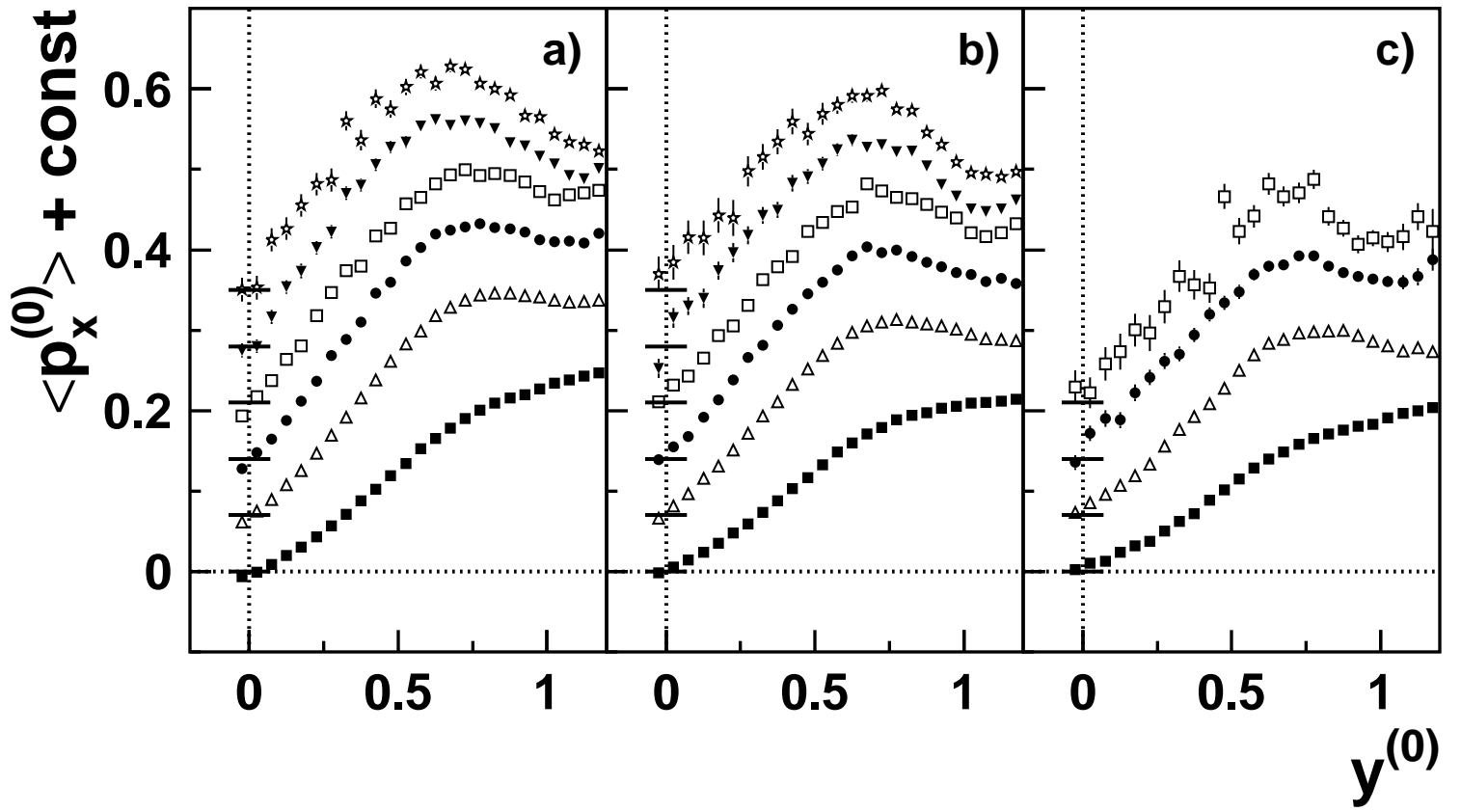


Figure 2

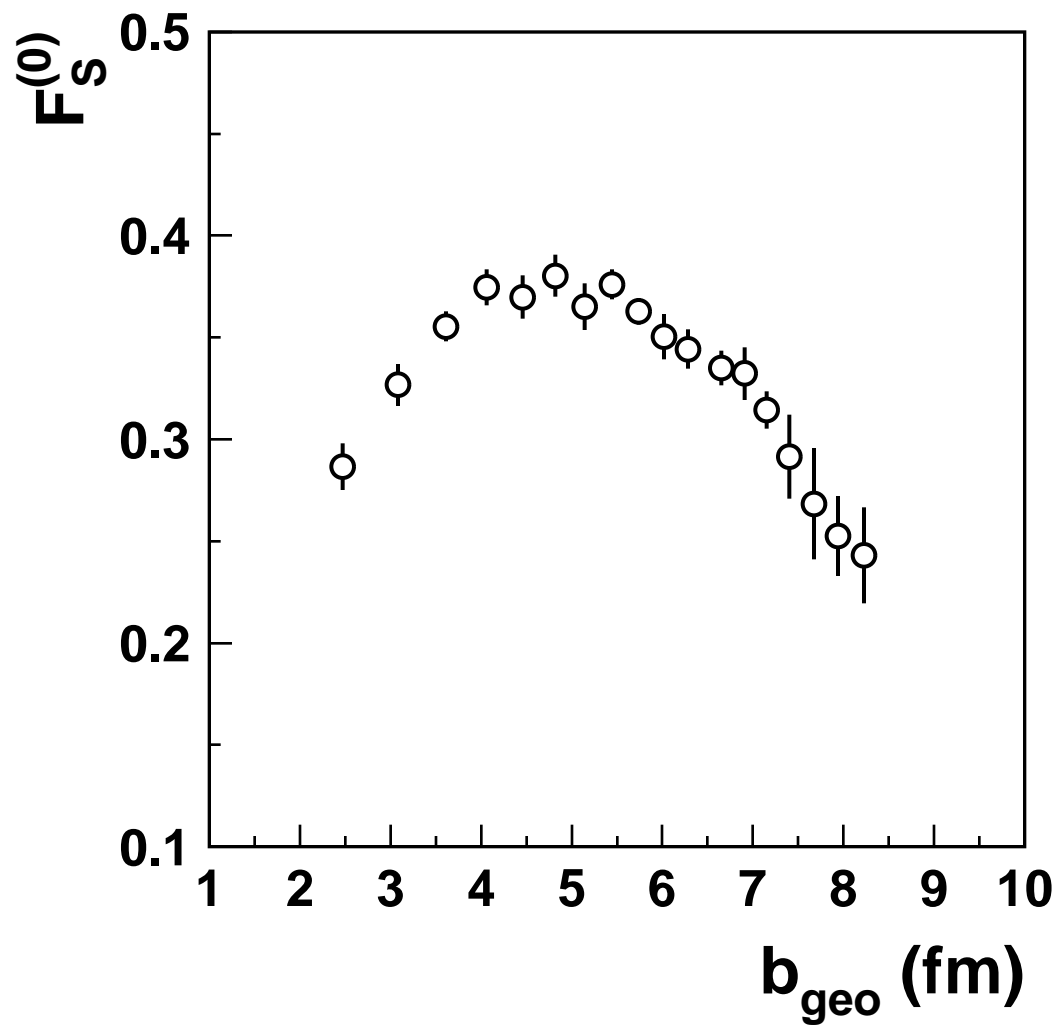


Figure 3

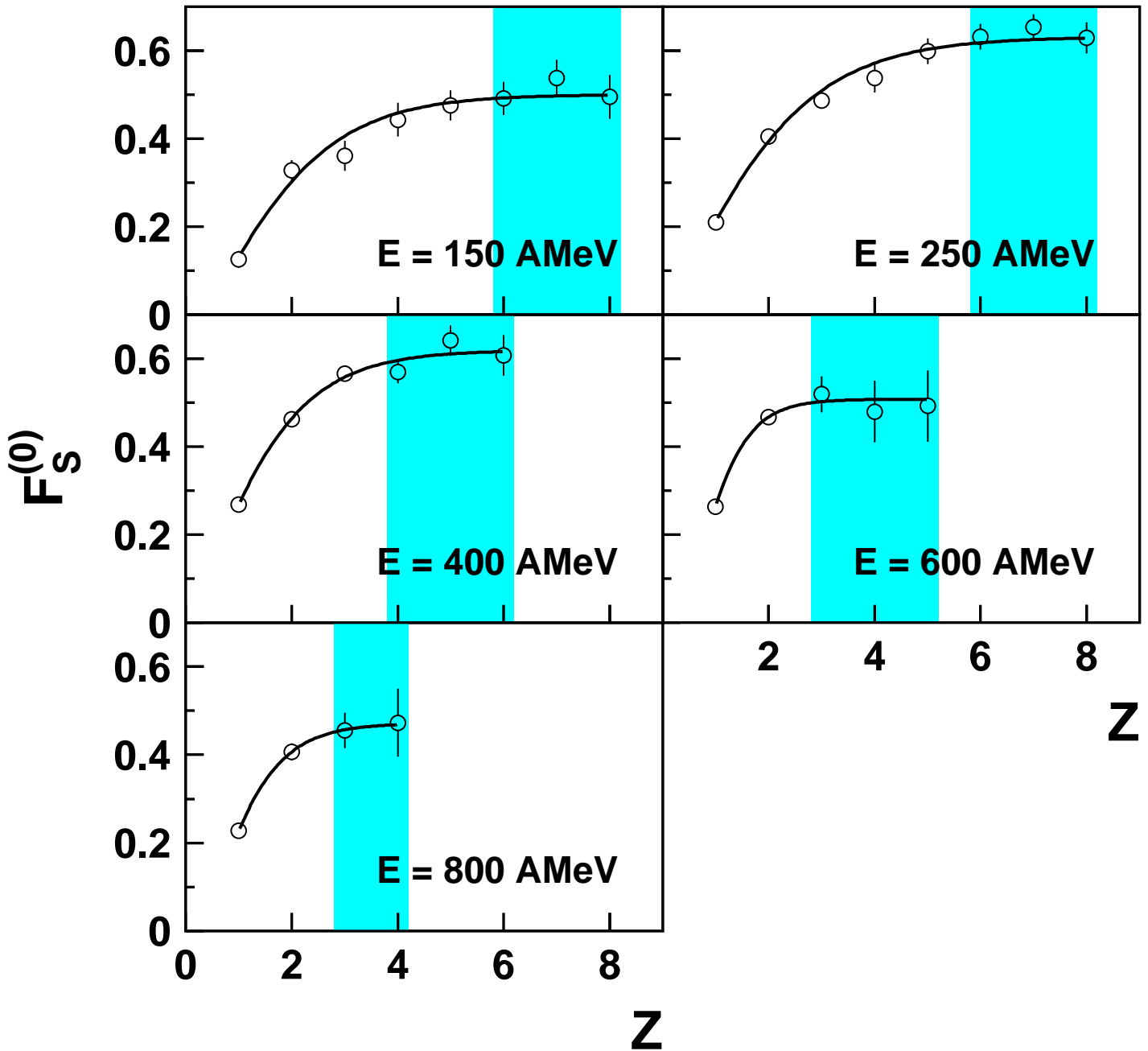


Figure 4

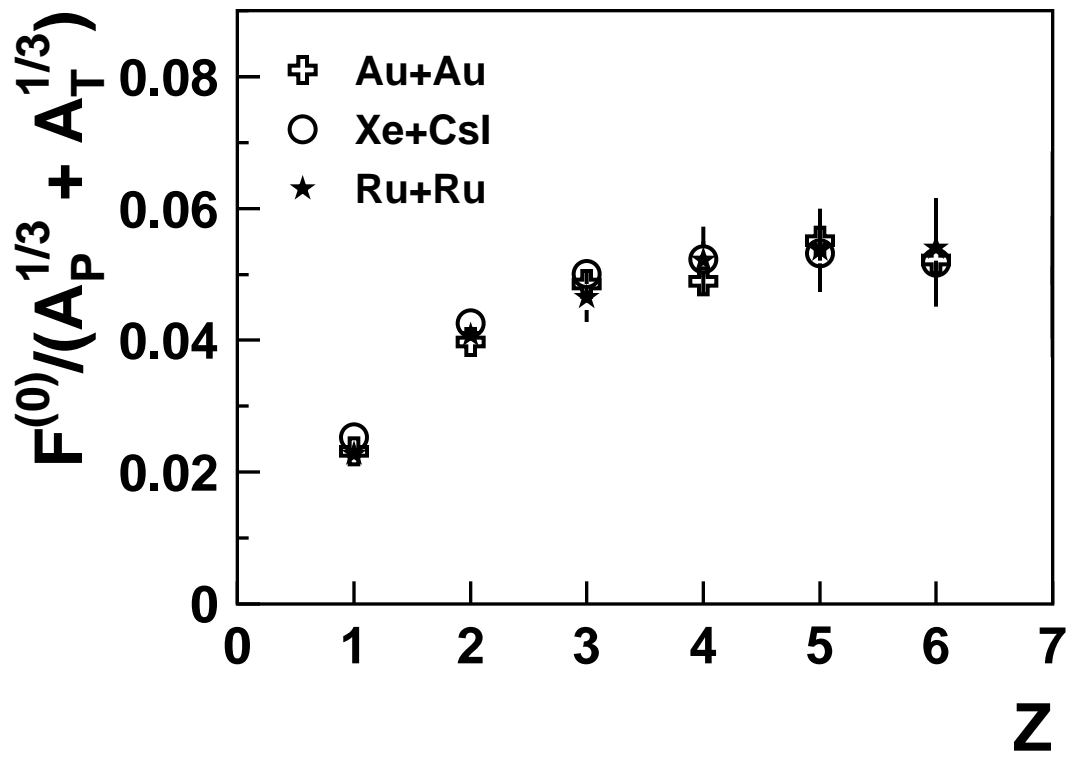


Figure 5

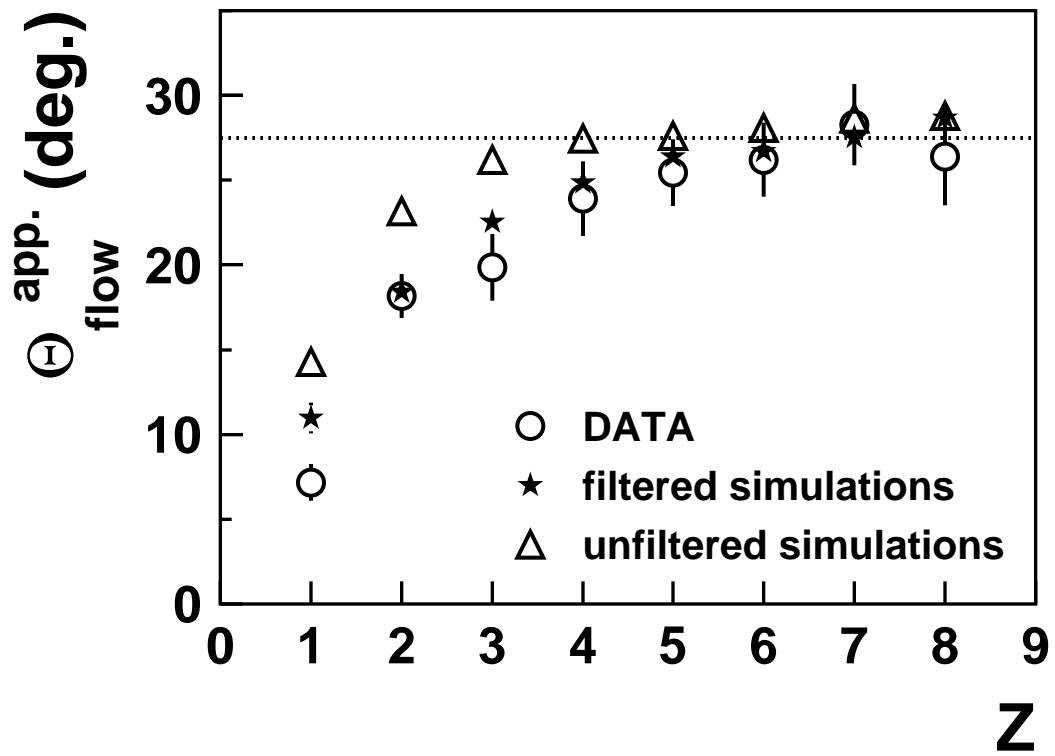


Figure 6

